



HAL
open science

Sorption of G-agent simulant vapours on human scalp hair

Clémentine Côte, Anne Piram, Alexandre Lacoste, Denis Josse, Pierre Doumenq

► **To cite this version:**

Clémentine Côte, Anne Piram, Alexandre Lacoste, Denis Josse, Pierre Doumenq. Sorption of G-agent simulant vapours on human scalp hair. *Chemico-Biological Interactions*, 2020, 326, pp.109111. 10.1016/j.cbi.2020.109111 . hal-03141875

HAL Id: hal-03141875

<https://hal.science/hal-03141875>

Submitted on 26 Feb 2021

HAL is a multi-disciplinary open access archive for the deposit and dissemination of scientific research documents, whether they are published or not. The documents may come from teaching and research institutions in France or abroad, or from public or private research centers.

L'archive ouverte pluridisciplinaire **HAL**, est destinée au dépôt et à la diffusion de documents scientifiques de niveau recherche, publiés ou non, émanant des établissements d'enseignement et de recherche français ou étrangers, des laboratoires publics ou privés.

Sorption of nerve agent simulants vapors on human scalp hair

1 **Authors**

Clémentine Côte ^a

Anne Piram ^a

Alexandre Lacoste ^b

Denis Josse ^c

Pierre Doumenq ^a

2 **Affiliations**

a. Aix Marseille Univ, CNRS, LCE, Marseille, France

b. Bataillon des Marins-Pompiers de Marseille, Marseille, France

c. Service Départemental d'Incendie et de Secours des Alpes-Maritimes SDIS06, Villeneuve-Loubet, France

3

4

5

1 Abstract

Human scalp hair is a biological matrix that can trap chemical vapors from explosives (TNT), drugs (THC) and chemical weapons (yprite). The external contamination of human's hair following exposure to organophosphorus (OP) nerve agent was simulated by model compounds: triethyl phosphate (TEP) and diisopropyl fluorophosphate (DFP). In this work were exposed strands of hair to vapors of TEP and DFP (3 and 7 ppm_v) to model sorption kinetics. Sorption isotherms were also investigated at several contamination levels (80 to 3000 mg.min.m⁻³). So following hair exposure extractions of OP nerve agent simulants from hair were conducted by soaking in 5 mL of DCM for 10 minutes under orbital mixing. Raw extracts were analyzed in GC-MS/MS to quantify each simulant content in hair. To conclude results are fitted by applying isotherm or kinetic equations and the best model is bimodal first-order to fit kinetic data, suggesting the co-existence of two different mechanisms of sorption. The best equation to describe OP vapors incorporation on hair is Freundlich model. Thus hair can be used as a passive sensor able to trap chemical warfare agents and can also offer valuable information regarding both individual contamination and proof of exposure to chemical weapons.

2 Keywords

Chemical warfare agents, triethyl phosphate, diisopropyl fluorophosphate, G-agents, passive sensor

Abbreviations

CWA Chemical warfare Agent

DCM Dichloromethane

DFP Diisopropyl fluorophosphate

OP Organophosphorus

PFO Pseudo-first-order

TEP Triethyl phosphate

Funding

This work was supported by the Direction Générale de l'Armement and Aix-Marseille University through a PhD grant.

1 **1. Introduction**

2 Chemical warfare agents (CWA) are highly toxic substances whose properties have been used
3 to kill, injure or incapacitate people during conflicts or terrorist attacks [1,2]. The issues surrounding
4 chemical weapons are not new. Indeed from ancient Greece (431-404 b.c.) during Peloponnesian
5 Spartans used ignited pitch and sulphur at Plataea and Delium [3,4]. In 1675 the first agreement was
6 signed by Germany and France in Strasbourg (France) to ban the use of poisoned bullets [1,3].
7 Various CWA including phosgene, yperite and lewisite were widely employed during World War I
8 and caused 100'000 deaths and 1.2 million injured people. Subsequently, during World War II,
9 millions of innocent civilians were killed in concentration camps by carbon monoxide, hydrogen
10 cyanide and Zyklon B. For the 1970s people use more the chemistry on the weapons and their
11 potential damage to fight [2,3,5]. To have an operational global control, Organisation for the
12 Prohibition of Chemical Weapons was entered into force in 1997, implementing Chemical Weapons
13 Convention [6]. This convention was ratified definitively by 192 Member States through the world
14 in October 2015 (some of other countries still negotiate about it nowadays) and they promised to stop
15 the development, the production, the storage and the use of all chemical weapons [7]. Unfortunately
16 exposures to CWA recently occurred [8]. The threat of use of chemical agents has not been
17 permanently ruled out and has been proved during conflicts (Syria, 2013) [9], terrorist attacks (Tokyo
18 subway, 1995) [9,10], assassinations (Kim Jong-Nam, 2017) [11] and assassination attempts (Skripal,
19 2018) [12].

20
21 The organophosphorus (OP) nerve agents are the largest group of CWA and are highly toxic
22 substances [13–17] because they exhibit lethal doses of exposures (LCT_{50}) lower than $400 \text{ mg}\cdot\text{min}\cdot\text{m}^{-3}$
23 ³ and they inhibit the enzyme acetylcholinesterase (AChE) which is the primary enzyme responsible
24 for the hydrolytic metabolism of the neurotransmitter acetylcholine (ACh) into choline and acetate.
25 That causes the accumulation of acetylcholine in the cholinergic synapses [18]. The first clinical signs
26 of OP nerve agents poisoning are the appearance of headaches, breathing difficulties and miosis (if
27 the eyes are exposed). In the hardest cases are noticed important clinical signs : muscular paralysis,
28 hypersalivation and death by asphyxia [19].

29
30 An exposure to CWA can be proved by using biological matrices such as blood and urine
31 [18]. But their usages are limited to a very short time frame (2-3 days in urine and a few weeks in
32 blood) what restricts their utilization as a proof of CWA exposure for living persons. Then the key
33 point of this work is the identification of a sensor that could confirm an exposure to CWA after a long
34 period. For this purpose human scalp hair is an interesting alternative compared to blood and to urine

1 hair. In fact hair has been already used to demonstrate the drug consumption or the toxin exposure
2 months and sometimes years after the occurrence [20–22]. Thus the detection time frame of
3 contaminants in hair can be significantly increased compared to blood and to urine [20].
4

5 The hair surface area is estimated at $0.40 \text{ m}^2 \cdot \text{g}^{-1}$ [23]. The accessible surface on hair depends
6 on the amount available (5-200 g on average) and consequently hair offers an accessible surface
7 from 2 to 80 m^2 . As a comparison, in previous studies, the unprotected naked skin surface (head,
8 neck, arms and hands) was 0.48 m^2 and the full-body surface is on average 1.8 m^2 for a uniformed
9 soldier [24,25]. Thus the advantage of the hair surface area admit to achieve high sampling rate and
10 then low detection limits. Scalp hair can bring information about exogenous contamination and can
11 offer a valuable diagnostic tool to prove that a suspect was or is still in contact with illicit substances
12 [26–29]. This concept was developed by Spiandore et al. who showed sulfur mustard simulant is
13 detected in hair after exposure to vapors [30–32]; and by Oxley et al. who showed military explosive
14 compounds adsorb on hair [33–35].
15

16 It is compulsory to practice decontamination after an exposure to CWA or industrial toxics in
17 order to decrease the risk of adverse health effects for healthcare professionals and all people around.
18 In the UK Chilcott and al. (2018) proposed for the first time a protocol to integrate the hair
19 decontamination after an individual exposure to liquid or to particulate substances of CWA and toxic
20 industrial. That is why decontamination material should be used to clean head including hair and face
21 before doing a protocol for hands and all potentially exposed area [36].
22

23 Investigations were performed with surrogates that are able to mimic chemical and/or physical
24 interactions with hair of the real G-agents – one of OP nerve agent chemical classes – to determine
25 the ability of hair to trap OP nerve agents. This work focuses on the hair external contamination only
26 through vapors allowing to check the quantity adsorbed on the surface of hair and to evaluate sorption
27 kinetics and sorption isotherms. In this case the incorporation of vapors of triethyl phosphate (TEP)
28 and diisopropyl fluorophosphate (DFP) on hair was examined.
29

30 **2. Materials and methods**

31 **2.1. Chemicals, reagents and sample collection**

32 Analytical grade dichloromethane ($\text{DCM} \geq 99.8 \%$) was purchased from Merck (VWR,
33 France). Triethyl phosphate (TEP) (CAS No. 78-40-0) and diisopropyl fluorophosphate (DFP) (CAS
34 No. 55-91-4) were supplied by Sigma Aldrich. Working solutions were prepared by dissolving TEP

1 and DFP separately into DCM (0.5 mg.mL⁻¹). Natural blond hair strands (30 cm length) were obtained
2 from Secher-Fesnoux (Chaville, France).

3 2.2. Sorption experiments and extraction process

4 First, a 150 mg hair strand (around 5 cm length) was hung in the center of a 1 L round-
5 bottomed flask. Next the contaminant (working solution) was separately added and was evaporated
6 by gentle heating. Then the experiment was placed in a thermostated bath (20 °C).

7 Second, sorption kinetics were evaluated over 1 hour by exposing scalp hair strands to 50 µL
8 (50 mg.min.m⁻³ to 1500 mg.min.m⁻³) and 100 µL (100 mg.min.m⁻³ to 3000 mg.min.m⁻³) of working
9 solutions. Each experiment was performed in duplicate (n=2).

10 Third, sorption isotherms were performed over 30 minutes, scalp hair strands were exposed
11 to simulant vapors emitted by 5 to 200 µL of working solutions (80 mg.min.m⁻³ to 3000 mg.min.m⁻³).
12 Each experiment was performed in triplicate (n=3).

13 Finally, at the end of the simulant exposure every hair extraction was conducted by soaking hair
14 in 5 mL of DCM for 10 minutes under orbital mixing at a shaking speed of 250 rpm in order to
15 succeed in this experiment.

16

17 2.3. Analytical method

18 1000 µL of raw extract was spiked with 10 µL of an internal standard (50 µg.mL⁻¹ in DCM).
19 TEP was used as internal standard for DFP sorption experiments, and DFP was used as internal
20 standard for TEP. The concentrations of each simulant content in hair (q_t) were determined by GC-
21 MS/MS analysis. The amount (q_t) of simulant adsorbed per mass unit of hair (µg.g⁻¹) was calculated
22 according to Eq. (1).

$$23 \quad q_t = C_t \times \frac{V}{m} \quad (1)$$

24 Where C_t and V are respectively the concentration (µg.mL⁻¹) and the volume (mL) of raw extract
25 and m is the mass of hair strands (g).

26

27 The analyses were performed by Gas Chromatography (7890A Agilent Technologies) coupled
28 to tandem Mass Spectrometer (7000 Agilent Technologies) equipped with an autosampler (7693,
29 Agilent Technologies). The separation was carried out on HP5-MS column (5%-phenyl, 95%
30 dimethylpolysiloxane; 30 m × 0.25 mm × 0.25 µm) with a constant Helium flow rate of 1 mL.min⁻¹.
31 For each analysis, 1 µL of the solution was injected into the injector at 250 °C in a splitless mode
32 with a purge time of one minute. The oven temperature program was applied as follows: 1 min at

1 50 °C, then the temperature increases at a rate of 100 °C.min⁻¹ in order to arrive to 80 °C held for 2
 2 min then new temperature ramp at 20 °C.min⁻¹ in order to arrive to 280 °C as a final temperature and
 3 held for 3 min for a complete run of 16.3 minutes with a solvent delay at 4 min. The transfer line was
 4 maintained at 260 °C and the mass spectrometer was equipped with an Electron Impact (EI, 70 eV)
 5 ionization source at 230 °C and two quadrupole analyzers at 150 °C. The mass transitions were
 6 performed in multiple reactions monitoring (MRM) mode and detection parameters were optimized
 7 and are summarized in Table 1.

8 *Table 1 : Fragmentation and detection parameters used for target compounds (retention time, MRM quantifier and qualifier transitions*
 9 *and collision energies)*

Compound	Retention time (min)	Transitions for Quantification			Transitions for Qualification		
		Precursor ion (m/z)	Product ion (m/z)	CE (V)	Precursor ion (m/z)	Product ion (m/z)	CE (V)
TEP	6.35	154.9	98.9	10	154.9	127.0	2
DFP	4.60	126.9	100.9	10	140.9	101.0	5

10

11 2.4. Quality assurance

12 A quality control procedure was constructed to ensure the reproducibility of the analytical
 13 method. For each analytical sequence a calibration curve (0.5 to 2000 ng.mL⁻¹) was carried out with
 14 a minimum of 6 points (R² > 0.99 and ± 10 % accuracy of each standard). Samples were separated
 15 by solvent blanks (DCM) in order to control the absence of cross contamination. A quality control
 16 solution was injected every 12 samples. Their concentrations were back calculated from the
 17 calibration curve in order to check the accuracy of the method. The unspiked human hair scalps were
 18 also analyzed to check the absence of carryover in blank contamination. The target compounds have
 19 never been detected.

20 Instrumental detection and quantification limits (LOD and LOQ) were determined with a
 21 standard solution and by calculating respectively a signal to noise ratio (S/N) of three and ten (Table
 22 2). The sample's quantification was possible above 0.4 and 0.04 ng.mL⁻¹. So we can detect values
 23 until 0.02 µg.g⁻¹ for TEP and 0.002 µg.g⁻¹ for DFP. The Method Quantification Limit (MQL) was
 24 estimated following Eq. (2):

$$25 \quad MQL = 5 \times \frac{LOQ}{m} \quad (2)$$

26 Where LOQ is the instrumental quantification limit and m the mass of the strand of hair (Table 2). In
 27 this work uncertainties to each measurement point correspond to 3 times the standard deviation.

28

1 *Table 2 : Quality parameters of the analytical method*

Compound	LOD (ng.mL ⁻¹)	LOQ (ng.mL ⁻¹)	MQL (µg.g ⁻¹)
TEP	0.12	0.4	0.02
DFP	0.01	0.04	0.002

2

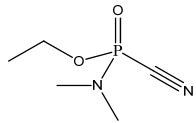
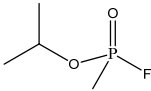
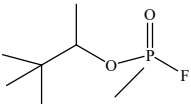
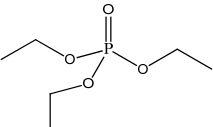
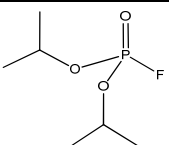
3 **3. Results and discussion**

4 **3.1. Choice of simulants for G-agents**

5 This work was carried out with simulants due to the toxicity and restriction of the OP nerve
 6 agents utilization [19,37]. The selection of compounds that can correctly mimic OP nerve agent
 7 behaviors in gas phase and their interactions with human's hair was then crucial. So, in order to
 8 extrapolate our results to G-agents, an important attention is given to the analysis of similarities
 9 concerning physico-chemical properties (vapor pressure, Henry constant and partition coefficient) or
 10 chemical structure (Table 3). As claimed by Bartelt-Hunt et al. a single simulant cannot mimic all G-
 11 agents properties [38].

12 Thus, two specific simulants were carefully selected to better cover physical and chemical
 13 properties of OP G-agents: TEP and DFP. They both have been often used as G-agent simulants [38]
 14 and they present a semi-persistent behavior as G-agents because of their volatility (Table 3). The use
 15 of TEP (VP = 0.39 mmHg) and DFP (VP = 0,519 mmHg) are in good agreement with G-agent's
 16 volatility (range 0.057 – 2.74 mmHg). Furthermore values of octanol-water partition coefficients for
 17 G-agents are between 0.299 – 1.824 against 0.800 and 1.173 for TEP and DFP respectively. All the
 18 log K_{ow} are in the same range. Thus this value is an estimation of a chemical's trend to compare
 19 polarity to mimic interactions with the hair fiber. Their amphiphilic character involves rapid sorption,
 20 moderate storage, and therefore a rapid resorption in hair. They also present similar structures (C₂H₅-
 21 O-P=O; (C₃H₈)_{iso}-O-P=O) with G-agents (C₂H₅-O-P=O for Tabun ; (C₃H₈)_{iso}-O-P=O for Sarin) what
 22 allows to correctly mimic some chemical relationships with hair (Table 3). Moreover as shown in
 23 Table 3 Henry's law constant are in the same range as G-agents (1.5.10⁻⁷ - 5.7.10⁻⁷) and simulants
 24 (3.6.10⁻⁸ - 3.2.10⁻⁶).

Table 3 : Physical, chemical and toxicological properties of OP nerve agents and simulants [15–17,38–43]

	Compounds (Abbreviation)	Formula	Molecular Weight (g.mol ⁻¹)	Vapor pressure at 25 °C (mmHg)	Volatility (mg.m ⁻³)	Vapor density	log K _{ow}	H at 25°C (atm.m ² .mol ⁻¹)	LC ₅₀ (Inhalation) (mg.min.m ⁻³)	LD ₅₀ (mg/ a man of 70 kg)
G-agent	Tabun (GA) 	C ₅ H ₁₁ N ₂ O ₂ P	162.13	0.057	497	5.6	0.384±0.033	1.5.10 ⁻⁷	70-400	1500
	Sarin (GB) 	C ₄ H ₁₀ FO ₂ P	140.09	2.74	20 660	4.8	0.299±0.016	5.7.10 ⁻⁷	35-100	1700
	Soman (GD) 	C ₇ H ₁₆ FO ₂ P	182.17	0.4	3 900	6.3	1.824±0.109	4.7.10 ⁻⁶	35-70	350
G-agents simulant	Triethyl phosphate (TEP) 	C ₆ H ₁₅ O ₄ P	182.16	0.39	3 953	6.3	0.80	3.6.10 ⁻⁸	>8817 mg.m ⁻³ (for 4h-rat)	1.6 g.kg ⁻¹ (rat)
	Diisopropyl fluorophosphate (DFP) 	C ₆ H ₁₄ FO ₃ P	184.15	0.579 (20°C)	5 748	6.4	1.173±0.051	3.2.10 ⁻⁶		

3.2. Sorption kinetics

Hair contamination by TEP and DFP was evaluated immediately after the hair vapor exposure. The amounts of surrogate accumulated in hair at different time frames are presented in Figure 1. As expected TEP and DFP content in hair increased both with time of exposure and concentration of simulant in the vapor phase (Figure 1). It was noteworthy that even for very short exposure times (5 min) simulant residues have been quantified in a 150 mg hair strand. As a very small amount of hair is required to perform this analysis, scalp hair sampling could reasonably be performed on a victim in the theatre of operation.

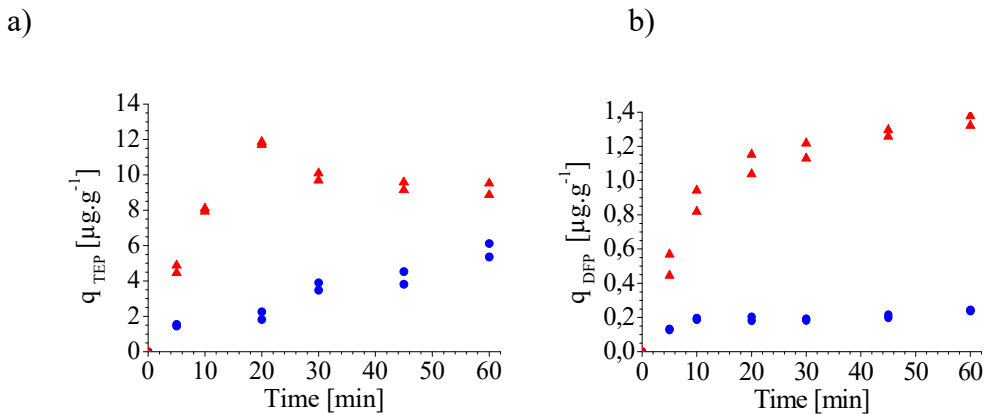


Figure 1 : TEP (a) and DFP (b) sorption kinetics on hair at 2 vapor concentrations: ● 3 ppm_v and ▲ 7 ppm_v

The amount of both simulants recovered in hair increased with exposure time. At 3 ppm_v exposure $1.50 \pm 0.2 \mu\text{g.g}^{-1}$ and $0.130 \pm 0.009 \mu\text{g.g}^{-1}$ were detected after five minutes of TEP and DFP exposure against $6 \pm 2 \mu\text{g.g}^{-1}$ and $0.24 \pm 0.01 \mu\text{g.g}^{-1}$ after one hour. At 7 ppm_v exposure $4.7 \pm 0.9 \mu\text{g.g}^{-1}$ and $0.5 \pm 0.3 \mu\text{g.g}^{-1}$ were detected after five minutes of TEP and DFP exposure against $9.2 \pm 1.5 \mu\text{g.g}^{-1}$ and $1.3 \pm 0.1 \mu\text{g.g}^{-1}$ after one hour. A plateau was observed after 30 min of exposure to 7 ppm_v TEP vapors what suggested an equilibrium reached state.

Data were fitted according to the most common kinetic models in order to assess the sorption mechanisms: pseudo-first-order (PFO) [44], bimodal first-order [45], Elovich [46] and intra-particle diffusion models [47].

The PFO equation based on Lagergren's model was widely used in sorption kinetics [48–50] which only involve the substrate concentration in the rate determining step. This model was generally applied over initial time of the sorption process (20-30 minutes) [44,51] and was used to experimental data as follows Eq.(3). This specific model was based on the sorption capacity of solids.

$$\ln (q_e - q_t) = \ln (q_e) - k_1 \cdot t \quad (3)$$

Where q_e and q_t ($\mu\text{g}\cdot\text{g}^{-1}$) represent simulant amount sorbed at equilibrium and at any time t (min) and k_1 is the PFO rate constant (min^{-1}).

It was therefore relevant to also consider the combination of multiple first order processes resulting from two regimes of sorption: one fast and the other slow. Then a bimodal first-order equation was applicable for our experimental data as follows Eq.(4) [52].

$$q_t = q_1 \cdot e^{-k_2 t} + q_2 \cdot e^{-k_3 t} + b \quad (4)$$

Where q_t ($\mu\text{g}\cdot\text{g}^{-1}$) represent simulant amount sorbed at any time t (min); q_1 and q_2 ($\mu\text{g}\cdot\text{g}^{-1}$) represent simulant amount partial sorbed at equilibrium; k_2 and k_3 are the bimodal first-order rate constant (min^{-1}) and b the intercept related to the sorption step.

Elovich equation was also another model often used to chemisorption data as follows Eq.(5) [46,53]. This model was an empirical equation: the applicable equation to experimental data was developed by Chien and Clayton [54].

$$q_t = \frac{1}{\beta} \ln(t) + \frac{1}{\beta} \ln(\alpha \cdot \beta) \quad (5)$$

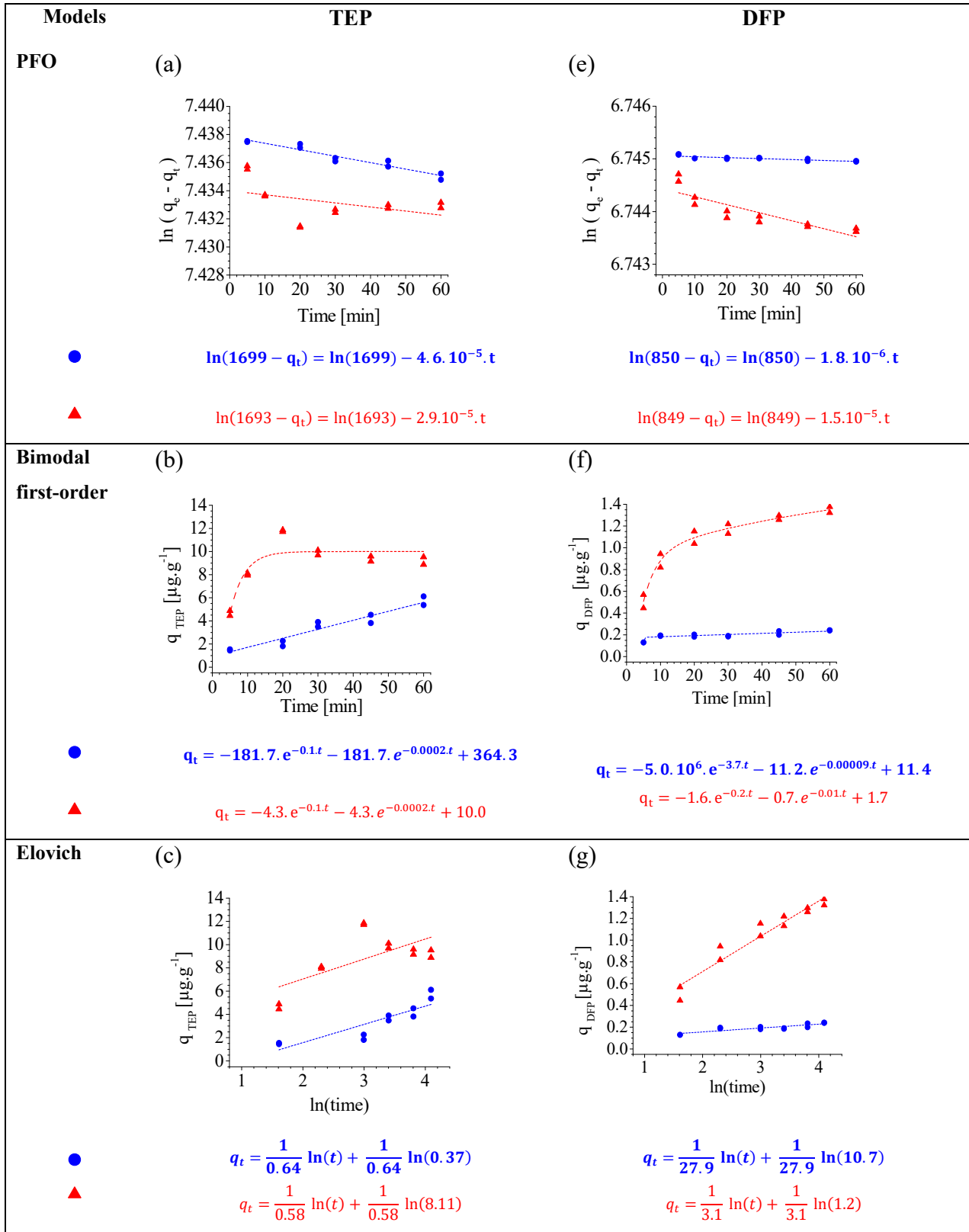
Where q_t ($\mu\text{g}\cdot\text{g}^{-1}$) represents simulant amount sorbed at any time t (min); α and β are respectively the initial rate ($\text{mg}\cdot\text{g}^{-1}\cdot\text{min}$) and the desorption constant during the experiments ($\text{mg}\cdot\text{g}^{-1}$).

Weber and Morris proposed also a model to describe internal diffusion [47] Eq.(6). This model was used to describe several reaction mechanisms such as surface diffusion and bulk diffusion [47,51].

$$q_t = k_i \cdot t^{1/2} + c \quad (6)$$

Where q_t ($\mu\text{g}\cdot\text{g}^{-1}$) represents simulant amount sorbed at any time t (min); k_i is the intraparticle diffusion rate constant ($\text{mg}\cdot\text{g}^{-1}\cdot\text{min}^{-1/2}$) and c is the intercept related to the sorption step.

A regression was applied for all models (Figure 2). The model relevance was evaluated by the determination coefficient (R^2) and the p-value in ANOVA tests (Table 4). The model that gave the highest determination coefficient and the lowest p-value was considered like the best to describe experimental data. All kinetic sorption equations were specified in Figure 2 and analysis parameters are determined (Table 4).



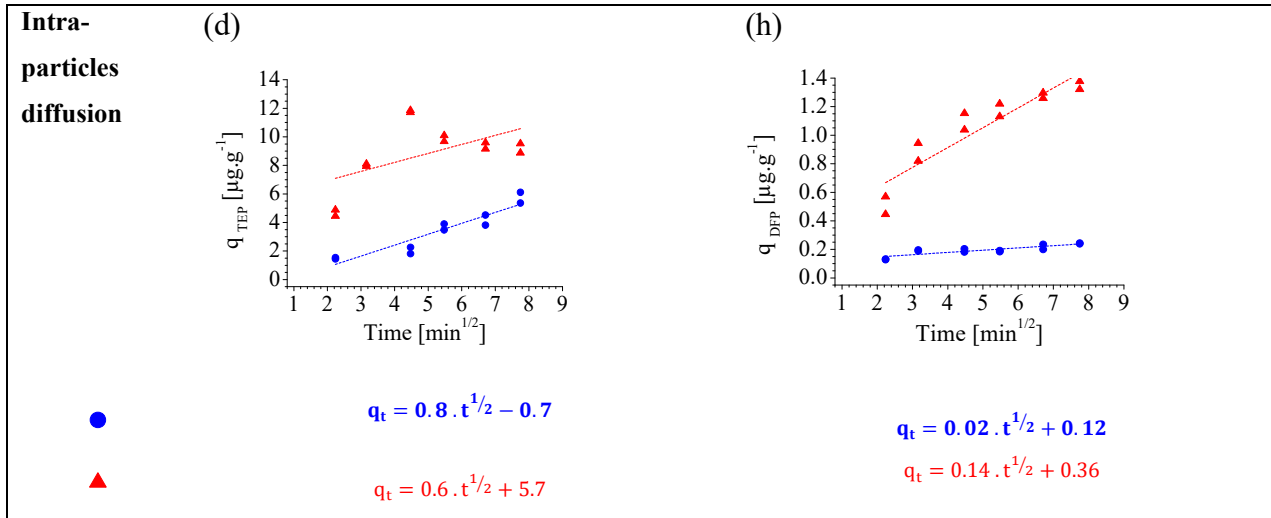


Figure 2 : Models for the sorption of TEP (a-d) and DFP (e-h) on hair; (a)(e) pseudo-first-order model, (b)(f) bimodal first-order, (c)(g) Elovich model and (d)(h) intraparticle diffusion model - ● 3 ppm_v and ▲ 7 ppm_v

Table 4 : Kinetic model parameters for TEP and DFP sorption on hair.

Models	Agents	TEP		DFP	
	Exposition	3 ppm _v	7 ppm _v	3 ppm _v	7 ppm _v
PFO	R ²	0.9192	0.1071	0.6703	0.7257
	p-value	7.5.10 ⁻⁶	0.1587	6.9.10 ⁻⁴	2.7.10 ⁻⁴
Bimodal first-order	R ²	0.8697	0.7162	0.8127	0.9551
	p-value	1.0.10 ⁻⁴	1.1.10 ⁻⁶	3.3.10 ⁻⁸	3.5.10 ⁻⁸
Elovich	R ²	0.7473	0.4043	0.7415	0.9309
	p-value	7.7.10 ⁻⁴	0.0156	2.0.10 ⁻⁴	2.5.10 ⁻⁷
Intra-particles diffusion	R ²	0.8662	0.2374	0.7154	0.8424
	p-value	5.8.10 ⁻⁵	0.0618	3.2.10 ⁻⁴	1.6.10 ⁻⁵

PFO, Elovich and intra-particle diffusion models were all rejected - considering sorption kinetics of TEP on scalp hair - because the determination coefficient R² was below 0.7. It was consequently considered that these models could not fit experimental data. The bimodal first-order fitting was presented a high determination coefficient above 0.7 at low and at high exposure doses (respectively 0.8697 and 0.7162). The nonlinear adjustments of the rate of time on the amount content in hair (q) as a function of time were led to a satisfactory coefficient of determination. Furthermore, the p-values were less than the significance level of 0.05 and the residues were randomly distributed according to this model what validates the relevance of this model.

Satisfactory results were obtained for all fittings with the DFP data excepted with the PFO for the experiment realized at 3 ppm_v. Indeed, we proved that the value of R² is not enough and that is

why it invalidated the relevance of this model. Furthermore, bimodal first-order, Elovich and intraparticle diffusion gave us acceptable coefficient of determination ($R^2 > 0.7$) and p-values (under the threshold value of 0.05). Bimodal first-order model described a better experimental data because it offered both the highest R^2 value and the lowest p-value as we observed for TEP.

The main differences between the two agents are volatility propriety and chemical structure (Table 1). Even though the volatility of TEP ($3\,953\text{ mg}\cdot\text{m}^{-3}$) is lower than this of DFP ($5\,748\text{ mg}\cdot\text{m}^{-3}$) but the amount of TEP found in hair is around ten times higher than this of DFP (Figure 1). For a given chemical compound this suggested an increase of the accumulation in hair with a decreasing volatility. Consequently, we could expect that low volatility G-agents could be more persistent in hair and should prove to us a less labile behavior. TEP and DFP volatilities are in the same range as G-agents ($497\text{-}20\,660\text{ mg}\cdot\text{m}^{-3}$): they are liquid at ambient temperature, and they all emit denser vapors than air (vapor density: 4.8-6.4).

All models described above (PFO, bimodal first-order, Elovich and intraparticle diffusion) are models that involve the combination of multiple sorption phenomena, either multilayered or both chemical and physical interactions which can be partly explained by the complexity of the scalp hair matrix. Indeed human hair is a natural fiber of α -keratin divided in three main components: cuticle, cortex and medulla - on average $50\text{-}100\ \mu\text{m}$ thickness - and has a specific elementary composition: around 51% carbon, 21% oxygen, 17% nitrogen and the rest are hydrogen and sulfur [55–57]. Furthermore the cortex is highly porous with various functional groups like carbonyl and amino groups [55,58]. So hair is a particularly complex substrate with an irregular and heterogeneous surface and hair-simulant interaction of different energies can coexist according to the nature of sorption sites. Besides several kinetics specific to each type of interaction can intervene in the sorption.

The acceptable correlation was observed for bimodal first-order for both simulants. The Elovich model brings to light the intra-particle diffusion and was often used to describe surface diffusion and bulk diffusion [47,51]. The heterogeneity of the hair surface [59] could lead to multiple interactions with OP nerve agent simulants depending on the position of the sorption site. Modeling by two sorption regimes from the hair can be coherent with this structure. Then we conclude that the sorption kinetics of OP nerve agent simulants is better represented by bimodal first-order model.

These two compounds TEP and DFP were both chosen to mimic nerve organophosphorus G-agents compartment. Thus it is reasonable to deduce and to assume that G-agents vapors will be trapped by hair and that the quantity recovered in hair will increase with the time of exposure. These

results prove us that hair can be used as a passive sensor and bring some information about OP nerve agents vapor exposure.

3.3. Sorption Isotherms

Hair contamination by TEP and DFP vapors were revealed by hair extraction immediately after exposure. Sorption isotherms were conducted at 20 °C for a fixed exposure time (30 minutes). As we expected TEP and DFP content in hair increased with concentration of simulant in the vapor phase. The amounts of simulant accumulated in hair along doses of exposure are presented in Figure 3. It is noteworthy that even for very short doses of exposure (0.02 Pa) simulant residues were quantified in hair (0.02±0.01 and 0.006±0.003 µg.g⁻¹ for TEP and DFP). The sorption isotherms of TEP and DFP were investigated.

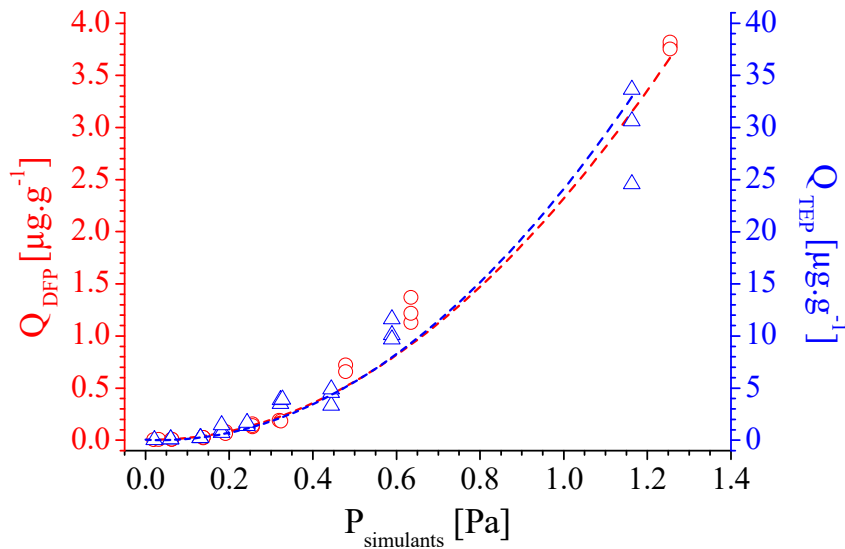


Figure 3 : Effects of TEP (Δ) and, DFP (O) sorption capacity on hair at different initial dose at vapor exposure after 30 minutes of exposure ($n=3$)

The isotherm data were fitted by applying the Langmuir and Freundlich isotherm relations. The Langmuir model is commonly used on sorption isotherms and the linear equation form is shown in Eq.(7) [51,60] and also applied recently by Wang and al [61].

$$\frac{C_e}{q_e} = \frac{1}{Q_{max}^0} C_e + \frac{1}{Q_{max}^0 + K_L} \quad (7)$$

Where q_e ($\mu\text{g.g}^{-1}$) represents simulant amount sorbed; C_e (Pa) is simulant amount exposed; Q_{max}^0 ($\mu\text{g.g}^{-1}$) is the maximum saturated monolayer sorption capacity of sorbent and K_L (Pa) is a constant related to the affinity between a sorbent and a sorbate.

The Freundlich model is one of the most commonly used equilibrium relations to describe heterogeneous systems [62,63]. The linear form is described by Eq.(8).

$$\log(q_e) = \log(k_f) + \frac{1}{n} \cdot \log(C_e) \quad (8)$$

Where q_e ($\mu\text{g}\cdot\text{g}^{-1}$) represents simulant amount sorbed; C_e (Pa) is simulant amount exposed, k_f is the Freundlich constant ($\mu\text{g}\cdot\text{g}^{-1}\cdot\text{Pa}^{-n}$), the sorption capacity of the sorbent and $1/n$ without dimension represents the heterogeneity factor to sorption intensity.

A linear regression was applied (Figure 4) for all models and the model relevance were evaluated with the determination coefficient (R^2) and the p-value in ANOVA test.

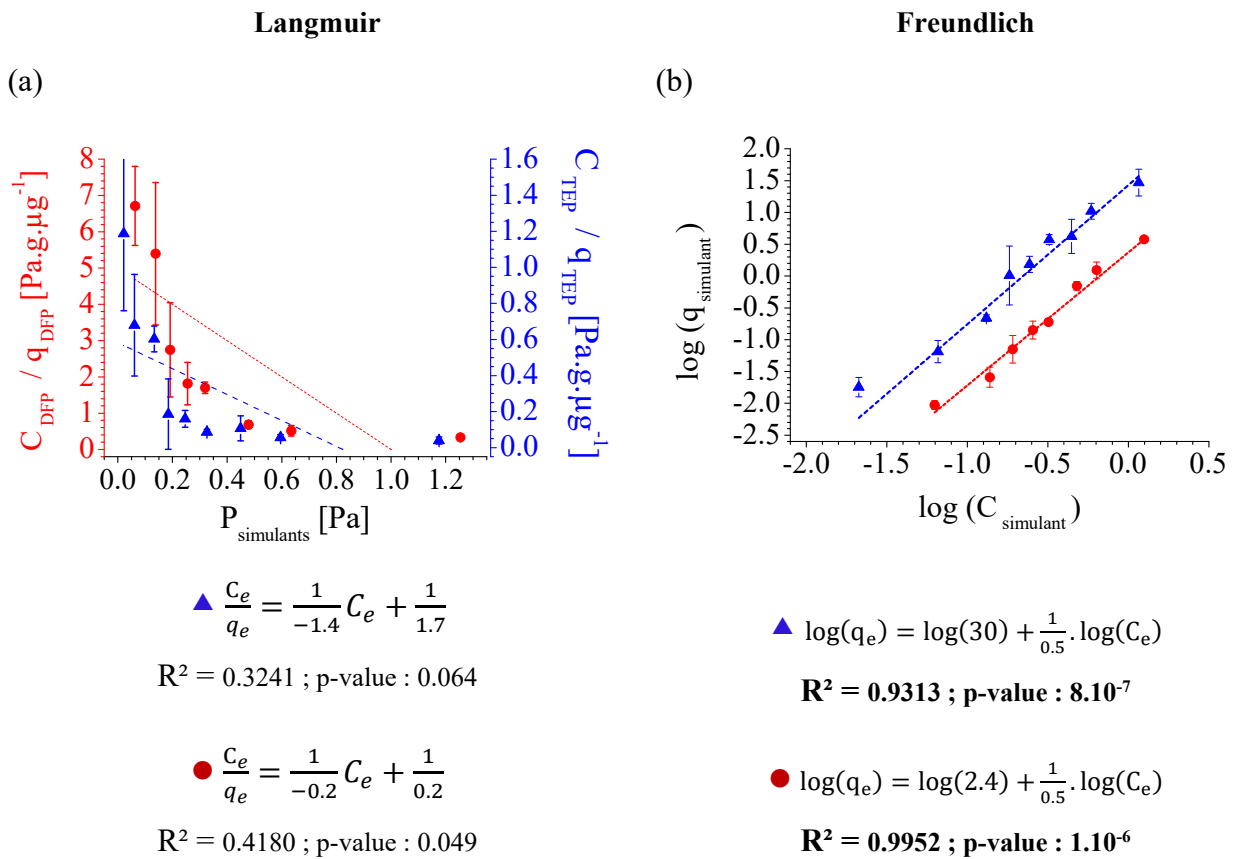


Figure 4 : Langmuir (a) and Freundlich (b) models for the sorption of TEP (▲) and DFP (●) on hair

The Langmuir model is obviously rejected for the fitting of TEP and DFP isotherms ($R^2 < 0.7$) as we illustrated in Figure 4. Moreover following regression equations and outlier results are obtained for Q_{\max}^0 , because we measured negative values and it is abnormal (-1.4 and $-0.2 \mu\text{g}\cdot\text{g}^{-1}$ respectively for TEP and DFP). Nonetheless the Freundlich model presents a good representativeness with all compounds as illustrated in Figure 4. For this model the determination coefficients are for us pretty

good (0.9313 and 0.9952) and the p-values are less than the significance level of 0.05 (8.10^{-7} and 1.10^{-6}). The linear adjustments logarithmic of the amount detected in hair ($\log q$) as a function of logarithmic amount exposed ($\log C$) leads to validate this model for both simulants. Furthermore the Freundlich model is consistent for multilayer adsorptions and take into account the heterogeneity of the adsorbent that can be expected for hair substrate [61].

So the sorption isotherms of TEP and DFP are best fitted by the Freundlich model. The sorption of G-agents vapor on hair could have a similar behavior to these two simulants by extrapolation. Thus the contaminant levels detected could depend on the dose of exposure and the Freundlich model could be used to interpret the data when the hair is in contact with a G-agent.

Specific models offer a good and a better fitting for G-agents (bimodal first-order and Freundlich) reminding that we consider both models very important: sorption kinetic model and sorption isotherm model. Even if hair is a particularly complex substrate with an irregular and heterogeneous surface we can see that hair-simulants interactions of different energies can coexist according to the sorption sites. Our findings show that hair can be used as a passive sensor for organophosphorus substances despite the complexity of this matrix. The G-agents simulants TEP and DFP could be identified and quantified in hair when exposure concentrations were close to the G-agents LC_{t50} .

We demonstrated that after vapor exposure to OP comprised between 80 and 3000 $mg \cdot min \cdot m^{-3}$ hair analysis can offer a valuable diagnostic tool for the identification of OP and an evaluation of the level of contamination in this study. In fact hair analysis can provide both qualitative and quantitative information even below the lethal dose. Finally hair samples could be used to diagnose an exposure to nerve agents.

Hair surface adsorption has already been investigated with other organic molecules, i.e. sulfur mustard [32], cannabinoids [26], cocaine [64] and explosives [33–35]. The hair capacity to trap external vapor contamination was demonstrated for all these target substances after a specific extraction procedure. Concerning Spiandore et al. (2014), they worked on a useful procedure for sulfur mustard detection on hair - another CWA. Their project underlined the hair capacity to trap CWA vapor and confirmed our statement: the intensity and the time of exposure are crucial. However the kinetic and isothermal models assigned were different. In their researches they were applied a pseudo- second-order equation and Langmuir isotherm model what implies a variable affinity with

the hair for OP nerve agents and sulfur mustard. These variations are easily explained by their own structure and physicochemical properties which generate variable behaviors with human's hair. All these and their results encouraged us to use hair as a passive sensor for CWA and identification of these agents following an individual exposure.

Finally all the data obtained in our work allow us to get information of the sorption of OP nerve agents concerning human's hair which are important for exposure risk assessments. Hair is able to capture a wide range of volatile compounds and various chemical properties (atmospheric pollutants, chemical weapons) [27,31,32,34,35]. That is why we can affirm that during a chemical attack, exposed people's hair will capture these organic compounds and the detection of a G-agent would bring the proof that a specific OP nerve agent was used after hair sampling and analysis.

4. Conclusion

To summarize, external contamination of scalp hair are observed when hair is exposed to vapor simulants (3 and 7 ppm_v) for various times (80 to 3000 mg.min.m⁻³). This shows the usefulness of hair analysis as a proof of exposure to chemical weapons. The experimental results demonstrate that the amount of both simulants recovered in hair after different times of TEP and DFP exposure increases with exposure time. Results also show that sorption kinetics follows a bimodal first-order kinetic and that isotherms are fitted better when using the Freundlich model for both simulants. By extrapolation, we consider the sorption of G-agents vapor on hair similar of the two simulants (TEP and DFP).

Finally all the data obtained in our work allow us to get information of the sorption of OP nerve agents concerning human's hair which are important for exposure risk assessments. We demonstrated hair can be used especially to reveal an exposure or handling of prohibited substances like organophosphorus nerve agents and thus to offer valuable information for health and for security services.

5. Acknowledgments

The authors gratefully acknowledge the DGA (Direction Générale de l'Armement) and AMU (Aix-Marseille University) for this partnership and their financial support.

6. References

- [1] N.H. Johnson, J.C. Larsen, E. Meek, Chapter 2 - Historical Perspective of Chemical Warfare Agents A2 - Gupta, Ramesh C., in: *Handb. Toxicol. Chem. Warf. Agents Second Ed.*, Academic Press, Boston, 2016: pp. 7–15.
- [2] J.K. Smart, Chapitre 2 History of chemical and biological warfare : an american perspective, in: *Med. Asp. Chem. Biol. Warf.*, 1997: pp. 8–86.
- [3] L. Szinicz, History of chemical and biological warfare agents, *Toxicology*. 214 (2005) 167–181. <https://doi.org/10.1016/j.tox.2005.06.011>.
- [4] C. Bertrand, C. Ammirati, C. Renaudeau, *Risques chimiques: accidents, attentats*, Elsevier Masson, 2006.
- [5] J.P. Robinson, C.-G. Hedén, H. von Schreeb, *The Problem of Chemical and Biological Warfare*, Almquist & Wiksells, Stockholm, 1973.
- [6] V. Pitschmann, Overall View of Chemical and Biochemical Weapons, *Toxins*. 6 (2014) 1761–1784. <https://doi.org/10.3390/toxins6061761>.
- [7] OPCW, *Convention on the prohibition of the development, production, stockpiling and use of chemical weapons and on their destruction*, (2005).
- [8] R. Pita, J. Domingo, The Use of Chemical Weapons in the Syrian Conflict, *Toxics*. 2 (2014) 391–402. <https://doi.org/10.3390/toxics2030391>.
- [9] J. Bajgar, J. Fusek, J. Kassa, K. Kuca, D. Jun, Chapter 3 - Global Impact of Chemical Warfare Agents Used Before and After 1945 A2 - Gupta, Ramesh C., in: *Handb. Toxicol. Chem. Warf. Agents Second Ed.*, Academic Press, Boston, 2015: pp. 17–25.
- [10] T. Okumura, K. Taki, K. Suzuki, T. Yoshida, Y. Kuroiwa, T. Satoh, Chapter 4 - The Tokyo Subway Sarin Attack: Acute and Delayed Health Effects in Survivors A2 - Gupta, Ramesh C., in: *Handb. Toxicol. Chem. Warf. Agents Second Ed.*, Academic Press, Boston, 2015: pp. 27–35. <http://www.sciencedirect.com/science/article/pii/B978012800159200004X> (accessed October 11, 2016).
- [11] J. Patočka, WHAT KILLED KIM JONG-NAM? WAS IT THE AGENT VX?, *MMSL*. 86 (2017) 86–89. <https://doi.org/10.31482/mmsl.2017.013>.
- [12] J.A. Vale, T.C. Marrs, R.L. Maynard, Novichok: a murderous nerve agent attack in the UK, *Clin. Toxicol.* 56 (2018) 1093–1097. <https://doi.org/10.1080/15563650.2018.1469759>.
- [13] J. Bajgar, Laboratory diagnosis of organophosphates/nerve agent poisoning, *Klin Biochem Metab.* 13 (2005) 40–47.
- [14] J. Bajgar, Organophosphates/nerve agent poisoning: mechanism of action, diagnosis, prophylaxis, and treatment, *Adv. Clin. Chem.* 38 (2004) 151–216.
- [15] D.H. Ellison, *Handbook of Chemical and Biological Warfare Agents*, Second Edition, CRC Press, 2008. <http://www.crcnetbase.com/doi/book/10.1201/9781420003291> (accessed October 11, 2016).
- [16] S. Lillie, E. Hanlon, J. Kelly, Rayburn BB, Potential military chemical/biological agents and compounds. *Multiservices Tactics Techniques and Procedures.*, (2005). <http://handle.dtic.mil/100.2/ADA457455> (accessed October 20, 2016).
- [17] A. Watson, D. Opresko, R.A. Young, V. Hauschild, J. King, K. Bakshi, Chapter 9 - Organophosphate Nerve Agents A2 - Gupta, Ramesh C., in: *Handb. Toxicol. Chem. Warf. Agents Second Ed.*, Academic Press, Boston, 2015: pp. 87–109. <http://www.sciencedirect.com/science/article/pii/B9780128001592000099> (accessed October 7, 2016).
- [18] J. Bajgar, Laboratory examination nerve agent intoxication, *Acta Medica Hradec Kralove Czech Repub.* 56 (2013) 89–96. <https://doi.org/10.14712/18059694.2014.15>.

- [19] S. Vucinic, B. Antonijevic, A.M. Tsatsakis, L. Vassilopoulou, A.O. Docea, A.E. Nosyrev, B.N. Izotov, H. Thiermann, N. Drakoulis, D. Brkic, Environmental exposure to organophosphorus nerve agents, *Environ. Toxicol. Pharmacol.* 56 (2017) 163–171. <https://doi.org/10.1016/j.etap.2017.09.004>.
- [20] F. Pragst, M.A. Balikova, State of the art in hair analysis for detection of drug and alcohol abuse, *Clin. Chim. Acta.* 370 (2006) 17–49. <https://doi.org/10.1016/j.cca.2006.02.019>.
- [21] M.R. Moeller, P. Fey, H. Sachs, Hair analysis as evidence in forensic cases, *Forensic Sci. Int.* 63 (1993) 43–53. [https://doi.org/10.1016/0379-0738\(93\)90258-C](https://doi.org/10.1016/0379-0738(93)90258-C).
- [22] G.L. Henderson, Mechanisms of drug incorporation into hair, *Forensic Sci. Int.* 63 (1993) 19–29. [https://doi.org/10.1016/0379-0738\(93\)90256-A](https://doi.org/10.1016/0379-0738(93)90256-A).
- [23] Y. Hessefort, B.T. Holland, R.W. Cloud, True porosity measurement of hair: a new way to study hair damage mechanisms, *J. Cosmet. Sci.* 59 (2008) 303–315.
- [24] S.D. Baker, J. Verweij, E.K. Rowinsky, R.C. Donehower, J.H. Schellens, L.B. Grochow, A. Sparreboom, Role of body surface area in dosing of investigational anticancer agents in adults, 1991–2001, *J. Natl. Cancer Inst.* 94 (2002) 1883–1888.
- [25] R.M. Wester, H. Tanojo, H.I. Maibach, R.C. Wester, Predicted Chemical Warfare Agent VX Toxicity to Uniformed Soldier Using Parathion in Vitro Human Skin Exposure and Absorption, *Toxicol. Appl. Pharmacol.* 168 (2000) 149–152. <https://doi.org/10.1006/taap.2000.9028>.
- [26] W.F. Duvivier, R.J.P. Peeters, T.A. van Beek, M.W.F. Nielen, Evidence based decontamination protocols for the removal of external Δ^9 -tetrahydrocannabinol (THC) from contaminated hair, *Forensic Sci. Int.* 259 (2016) 110–118. <https://doi.org/10.1016/j.forsciint.2015.12.014>.
- [27] E.S. Emídio, V. de Menezes Prata, H.S. Dórea, Validation of an analytical method for analysis of cannabinoids in hair by headspace solid-phase microextraction and gas chromatography–ion trap tandem mass spectrometry, *Anal. Chim. Acta.* 670 (2010) 63–71. <https://doi.org/10.1016/j.aca.2010.04.023>.
- [28] M.M. Madry, K.Y. Rust, R. Guglielmello, M.R. Baumgartner, T. Kraemer, Metabolite to parent drug concentration ratios in hair for the differentiation of tramadol intake from external contamination and passive exposure, *Forensic Sci. Int.* 223 (2012) 330–334. <https://doi.org/10.1016/j.forsciint.2012.10.012>.
- [29] L. Tsanaclis, J. Nutt, K. Bagley, S. Bevan, J. Wicks, Differentiation between consumption and external contamination when testing for cocaine and cannabis in hair samples, *Drug Test. Anal.* 6 Suppl 1 (2014) 37–41. <https://doi.org/10.1002/dta.1623>.
- [30] M. Spiandore, M. Souilah-Edib, A. Piram, A. Lacoste, D. Josse, P. Doumenq, Desorption of sulphur mustard simulants methyl salicylate and 2-chloroethyl ethyl sulphide from contaminated scalp hair after vapour exposure, *Chemosphere.* 191 (2018) 721–728. <https://doi.org/10.1016/j.chemosphere.2017.09.124>.
- [31] M. Spiandore, A. Piram, A. Lacoste, P. Prevost, P. Maloni, F. Torre, L. Asia, D. Josse, P. Doumenq, Efficacy of scalp hair decontamination following exposure to vapours of sulphur mustard simulants 2-chloroethyl ethyl sulphide and methyl salicylate, *Chem. Biol. Interact.* (2016). <https://doi.org/10.1016/j.cbi.2016.07.018>.
- [32] M. Spiandore, A. Piram, A. Lacoste, D. Josse, P. Doumenq, Hair analysis as a useful procedure for detection of vapour exposure to chemical warfare agents: simulation of sulphur mustard with methyl salicylate, *Drug Test. Anal.* 6 (2014) 67–73. <https://doi.org/10.1002/dta.1659>.
- [33] J.C. Oxley, J.L. Smith, L.J. Kirschenbaum, S. Marimiganti, I. Efremenko, R. Zach, Y. Zeiri, Accumulation of Explosives in Hair—Part 3: Binding Site Study*, *J. Forensic Sci.* 57 (2012) 623–635. <https://doi.org/10.1111/j.1556-4029.2011.02020.x>.
- [34] J.C. Oxley, J.L. Smith, E. Bernier, J.S. Moran, J. Luongo, Hair as Forensic Evidence of Explosive Handling, Propellants Explos. Pyrotech. 34 (2009) 307–314. <https://doi.org/10.1002/prep.200700285>.

- [35] J.C. Oxley, J.L. Smith, L.J. Kirschenbaum, S. Maringanti, Accumulation of Explosives in Hair—Part II: Factors Affecting Sorption*, *J. Forensic Sci.* 52 (2007) 1291–1296. <https://doi.org/10.1111/j.1556-4029.2007.00567.x>.
- [36] R.P. Chilcott, J. Larner, H. Matar, UK's initial operational response and specialist operational response to CBRN and HazMat incidents: a primer on decontamination protocols for healthcare professionals, *Emerg. Med. J.* (2018) emermed-2018-207562. <https://doi.org/10.1136/emermed-2018-207562>.
- [37] OPCW, Fact sheet 7: Monitoring Chemicals with Possible Chemical Weapons Applications, (2016).
- [38] S.L. Bartelt-Hunt, D.R.U. Knappe, M.A. Barlaz, A Review of Chemical Warfare Agent Simulants for the Study of Environmental Behavior, *Crit. Rev. Environ. Sci. Technol.* 38 (2008) 112–136. <https://doi.org/10.1080/10643380701643650>.
- [39] S.E. Czerwinski, J.P. Skvorak, D.M. Maxwell, D.E. Lenz, S.I. Baskin, Effect of octanol:water partition coefficients of organophosphorus compounds on biodistribution and percutaneous toxicity, *J. Biochem. Mol. Toxicol.* 20 (2006) 241–6.
- [40] S.E. Czerwinski, D.M. Maxwell, D.E. Lenz, A Method for Measuring Octanol:water Partition Coefficients of Highly Toxic Organophosphorus Compounds, *Toxicol. Methods.* 8 (1998) 139–149. <https://doi.org/10.1080/105172398242961>.
- [41] N.B. Munro, S.S. Talmage, G.D. Griffin, L.C. Waters, A.P. Watson, J.F. King, V. Hauschild, The sources, fate, and toxicity of chemical warfare agent degradation products., *Environ. Health Perspect.* 107 (1999) 933–974.
- [42] National Research Council, Subcommittee On Acute Exposure Guideline Levels, Acute Exposure Guideline Levels for Selected Airborne Chemicals: Volume 3., National Academies Press, 2003.
- [43] B.C. Singer, A.T. Hodgson, H. Destailats, T. Hotchi, K.L. Revzan, R.G. Sextro, Indoor Sorption of Surrogates for Sarin and Related Nerve Agents, *Environ. Sci. Technol.* 39 (2005) 3203–3214. <https://doi.org/10.1021/es049144u>.
- [44] Y.S. Ho, G. McKay, A Comparison of Chemisorption Kinetic Models Applied to Pollutant Removal on Various Sorbents, *Process Saf. Environ. Prot.* 76 (1998) 332–340. <https://doi.org/10.1205/095758298529696>.
- [45] T.-Y. Li, L.-J. Bao, C.-C. Wu, L.-Y. Liu, C.S. Wong, E.Y. Zeng, Organophosphate flame retardants emitted from thermal treatment and open burning of e-waste, *J. Hazard. Mater.* 367 (2019) 390–396. <https://doi.org/10.1016/j.jhazmat.2018.12.041>.
- [46] L. Largette, R. Pasquier, A review of the kinetics adsorption models and their application to the adsorption of lead by an activated carbon, *Chem. Eng. Res. Des.* 109 (2016) 495–504. <https://doi.org/10.1016/j.cherd.2016.02.006>.
- [47] W.J. Weber, J.C. Morris, Kinetics of Adsorption on Carbon from Solution, *J. Sanit. Eng. Div.* 89 (1963) 31–60.
- [48] S. Azizian, Kinetic models of sorption: a theoretical analysis, *J. Colloid Interface Sci.* 276 (2004) 47–52. <https://doi.org/10.1016/j.jcis.2004.03.048>.
- [49] K. Vasanth Kumar, S. Sivanesan, Equilibrium data, isotherm parameters and process design for partial and complete isotherm of methylene blue onto activated carbon, *J. Hazard. Mater.* 134 (2006) 237–244. <https://doi.org/10.1016/j.jhazmat.2005.11.002>.
- [50] R.-L. Tseng, F.-C. Wu, R.-S. Juang, Characteristics and applications of the Lagergren's first-order equation for adsorption kinetics, *J. Taiwan Inst. Chem. Eng.* 41 (2010) 661–669. <https://doi.org/10.1016/j.jtice.2010.01.014>.
- [51] H.N. Tran, S.-J. You, A. Hosseini-Bandegharai, H.-P. Chao, Mistakes and inconsistencies regarding adsorption of contaminants from aqueous solutions: A critical review, *Water Res.* 120 (2017) 88–116. <https://doi.org/10.1016/j.watres.2017.04.014>.

- [52] E. Schuhfried, E. Aprea, L. Cappellin, C. Soukoulis, R. Viola, T.D. Märk, F. Gasperi, F. Biasioli, Desorption kinetics with PTR-MS: Isothermal differential desorption kinetics from a heterogeneous inlet surface at ambient pressure and a new concept for compound identification, *Int. J. Mass Spectrom.* 314 (2012) 33–41. <https://doi.org/10.1016/j.ijms.2012.01.013>.
- [53] F.-C. Wu, R.-L. Tseng, R.-S. Juang, Characteristics of Elovich equation used for the analysis of adsorption kinetics in dye-chitosan systems, *Chem. Eng. J.* 150 (2009) 366–373. <https://doi.org/10.1016/j.cej.2009.01.014>.
- [54] S.H. Chien, W.R. Clayton, Application of Elovich equation to the kinetics of phosphate release and sorption in soils., *Soil Sci. Soc. Am. J.* 44 (1980) 265–268.
- [55] R. Satish, A. Vanchiappan, C.L. Wong, K.W. Ng, M. Srinivasan, Macroporous carbon from human hair: A journey towards the fabrication of high energy Li-ion capacitors, *Electrochimica Acta.* 182 (2015) 474–481. <https://doi.org/10.1016/j.electacta.2015.09.127>.
- [56] B. Bhushan, *Biophysics of Human Hair: Structural, Nanomechanical, and Nanotribological Studies*, Springer Berlin Heidelberg, Berlin, Heidelberg, 2010.
- [57] C. Popescu, H. Höcker, Hair—the most sophisticated biological composite material, *Chem. Soc. Rev.* 36 (2007) 1282–1291. <https://doi.org/10.1039/B604537P>.
- [58] Y. Yu, W. Yang, B. Wang, M.A. Meyers, Structure and mechanical behavior of human hair, *Mater. Sci. Eng. C.* 73 (2017) 152–163. <https://doi.org/10.1016/j.msec.2016.12.008>.
- [59] C.R. Robbins, *Chemical and Physical Behavior of Human Hair*, Fifth Edition, Springer Berlin Heidelberg, Dordrecht, 2012.
- [60] I. Langmuir, THE ADSORPTION OF GASES ON PLANE SURFACES OF GLASS, MICA AND PLATINUM., *J. Am. Chem. Soc.* 40 (1918) 1361–1403. <https://doi.org/10.1021/ja02242a004>.
- [61] C. Wang, L. Boithias, Z. Ning, Y. Han, S. Sauvage, J.-M. Sánchez-Pérez, K. Kuramochi, R. Hatano, Comparison of Langmuir and Freundlich adsorption equations within the SWAT-K model for assessing potassium environmental losses at basin scale, *Agric. Water Manag.* 180 (2017) 205–211. <https://doi.org/10.1016/j.agwat.2016.08.001>.
- [62] H. M. F. Freundlich, “Over the Adsorption in Solution,” *The Journal of Physical Chemistry*, Vol. 57, 1906, pp. 385-471. - References - Scientific Research Publish, (n.d.). [http://www.scirp.org/\(S\(i43dyn45teexjx455qlt3d2q\)\)/reference/ReferencesPapers.aspx?ReferenceID=857464](http://www.scirp.org/(S(i43dyn45teexjx455qlt3d2q))/reference/ReferencesPapers.aspx?ReferenceID=857464) (accessed July 17, 2017).
- [63] Y.-S. Ho, Review of second-order models for adsorption systems, *J. Hazard. Mater.* 136 (2006) 681–689. <https://doi.org/10.1016/j.jhazmat.2005.12.043>.
- [64] W.L. Wang, E.J. Cone, Testing human hair for drugs of abuse. IV. Environmental cocaine contamination and washing effects, *Forensic Sci. Int.* 70 (1995) 39–51. [https://doi.org/10.1016/0379-0738\(94\)01616-D](https://doi.org/10.1016/0379-0738(94)01616-D).